Metal complexes of N-o-chlorobenzamido-meso-tetraphenylporphyrin: cis-Tl(N-NCO(o-Cl)C6H4-tpp)(OAc) and trans-Cd(N-NHCO(o-Cl)C6H4-tpp)(OAc) (tpp=5, 10, 15, 20-tetraphenylporphyrinat...

ARTICLE *in* INORGANIC CHEMISTRY COMMUNICATIONS · APRIL 2010

Impact Factor: 1.78 · DOI: 10.1016/j.inoche.2010.01.022

5 AUTHORS, INCLUDING:

Jyh-Horung Chen
National Chung Hsing University
86 PUBLICATIONS **649** CITATIONS

Inorganic Chemistry Communications 13 (2010) 506–510

Contents lists available at ScienceDirect

Inorganic Chemistry Communications

journal homepage: www.elsevier.com/locate/inoche

Metal complexes of N-*o*-chlorobenzamido-*meso*-tetraphenylporphyrin: *cis*-Tl(*N*-NCO(*o*-Cl)C_6H_4-tpp)(OAc) and *trans*-Cd(*N*-NHCO(*o*-Cl)C_6H_4-tpp)(OAc) (tpp = 5, 10, 15, 20-tetraphenylporphyrinate)

Kwan-Tin Chen [a], Ming Yang Tsai [a], Jyh-Horung Chen [a,*], Shin-Shin Wang [b], Jo-Yu Tung [c,*]

[a] Department of Chemistry, National Chung-Hsing University, Taichung 40227, Taiwan
[b] Material Chemical Laboratories, Hsin-Chu 300, Taiwan
[c] Department of Occupational Safety and Health, Chung Hwai University of Medical Technology, Tainan 717, Taiwan

ARTICLE INFO

Article history:
Received 14 December 2009
Accepted 28 January 2010
Available online 4 February 2010

Keywords:
Thallium
Cadmium
X-ray diffraction
N-Substituted-N-aminoporphyrin
Dynamic NMR

ABSTRACT

The crystal structures of diamagnetic (*cis*-acetato) (N-*o*-chlorobenzamido-*meso*-tetraphenylporphyrinato)thallium(III)·0.5 water solvate [*cis*-Tl(*N*-NCO(*o*-Cl)C_6H_4-tpp)(OAc)·0.5 H_2O; **3**·0.5 H_2O] and diamagnetic (*trans*-acetato) (N-*o*-chlorobenzamido-*meso*-tetraphenylporphyrinato)cadmium(II) methylene chloride solvate [*trans*-Cd(*N*-NHCO(*o*-Cl)C_6H_4-tpp)(OAc)·CH_2Cl_2; **4**·CH_2Cl_2] were determined. The coordination sphere around the Tl^{3+} (or Cd^{2+}) in **3** (or **4**) is a distorted square-based pyramid in which the apical site is occupied by a chelating bidentate OAc^- group. In **3**, Tl^{3+} and N(5) are located on the same side at 1.18 and 1.26 Å from it 3N plane, but in **4**, Cd^{2+} and N(5) are located on different sides at 1.06 and −1.55 Å from it 3N plane. The free energy of activation at the coalescence temperature T_c for the intermolecular acetate exchange process in **3** in CD_2Cl_2 solvent is found to be $\Delta G^{\neq}_{198} = 42.1$ kJ/mol through ^{1}H NMR temperature-dependent measurements. Likewise, the free energy of activation $\Delta G^{\neq}_{293} = 55.94$ kJ/mol is determined for the intramolecular exchange of the ortho protons between *o*′-H (34, 40) and *o*′-H (38, 44) in **3** in CD_2Cl_2. VT NMR (^{1}H and ^{13}C) studies of **4** show that the acetate acts as a bidentate ligand and the OAc^- exchange does not occur in CD_2Cl_2. Moreover, the NH proton [*i.e.*, H(5)] of **4** in CD_2Cl_2 is observed as a singlet at δ −0.09 ppm with $\Delta\nu_{1/2}$ = 13 Hz at 20 °C indicating that the NH protons undergo intermediate intermolecular proton exchange with water at this temperature.

Previously, we reported two-stage formation of (N-*o*-chlorobenzamido-*meso*-tetraphenylporphyrinato)(methanol)zinc(II) methanol solvate [Zn(*N*-NCO(*o*-Cl)C_6H_4-tpp)(MeOH)·MeOH; **1**·MeOH] [1]. Compound **1** is a zinc complex of *N*-NHCO(*o*-Cl)C_6H_4-Htpp) (**2**) (Chart 1). The absolute values of hardness η for Zn^{2+}, Tl^{3+} and Cd^{2+} are 10.88, 10.4, and 10.29 eV, respectively [2]. It is observed that the effective ionic radius (r) for the metal ion increases from 0.82 Å for Zn^{2+} (S = 0) with coordination number (CN) = 5 [or 1.025 Å for Tl^{3+} (S = 0) with CN = 6] to 1.09 Å for Cd^{2+} (S = 0) with CN = 6 [3]. In these three metal ions the polarizing power z/r^2 (z = charge on the cation, r = ionic radius) decreases from 3.652 (Zn^{2+}) [or (Tl^{3+})] to 2.041 (Cd^{2+}) [4,5]. The metal cations of different polarizing power selected were Tl^{3+} and Cd^{2+}. The soft acid Tl^{3+} with a larger polarizing power (2.855) similar to that of Zn^{2+} attacks the two N–H protons of **2** and lead to a six-coordinate distorted trigonal prismatic Tl (III) derivative, that is, (*cis*-acetato)(N-*o*-chlorobenzimido-*meso*-tetraphenylporphyrinato)thallium (III)·0.5 water solvate [Tl(*N*-NCO(*o*-Cl)C_6H_4-tpp)(OAc)·0.5 H_2O; **3**·0.5 H_2O] possessing a nitrene moiety inserted between the thallium atom and one nitrogen atom, N(4) (Scheme 1). During the metallation of free base **2** with $Cd(OAc)_2$, the soft acid Cd^{2+} with a lower polarizing power (2.041) prefers to retain one OAc^- ligand and coordinate to the N–H proton [*i.e.* H(2A)] of **2** also to form a six-coordinate distorted trigonal prismatic complex, that is, (*trans*-acetato)(N-*o*-chlorobenzimido-*meso*-tetraphenylporphyrinato)cadmium(II) methylene chloride solvate [*trans*-Cd(*N*-NHCO(*o*-Cl)C_6H_4-tpp)(OAc)·CH_2Cl_2; **4**·CH_2Cl_2] (Scheme 1). In this paper, we describe the X-ray structural investigation on the complexation of Tl^{3+} and Cd^{2+} classified as C acids (covalent acids) but with different polarizing power into **2** leading to mononuclear complexes of *cis*-**3** and *trans*-**4** [4,5]. In addition, the ^{1}H and ^{13}C NMR spectra of *cis*-**3** in CD_2Cl_2 at various temperatures are used to investigate the intermolecular apical ligand (OAc^-) exchange process and in turn to determine the free energy of activation at the coalescence temperature, $\Delta G^{\neq}_{Tc}$, for the exchange process.

* Corresponding authors. Tel.: +886 4 228 40411x612; fax: +886 4 228 62547 (J.H. Chen), tel.: +886 6 267 4567x815; fax: +886 6 289 4028 (J.Y. Tung).
E-mail addresses: JyhHChen@dragon.nchu.edu.tw (J.-H. Chen), joyuting@mail.hwai.edu.tw (J.-Y. Tung).

1387-7003/$ - see front matter © 2010 Elsevier B.V. All rights reserved.
doi:10.1016/j.inoche.2010.01.022

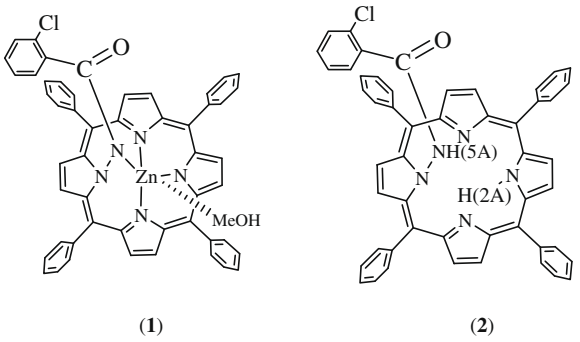

(**1**) (**2**)

Chart 1.

Using a d^{10} metal, namely, thallium(III) and cadmium(II), the new complexes **3** and **4** were synthesized. The synthetic strategy is outlined in Scheme 1. The complex *cis*-Tl(N-NCO(*o*-Cl)C_6H_4-tpp)(OAc) (**3**) was produced in 63% yield by heating a *N*-NHCO(*o*-Cl) C_6H_4-Htpp) (**2**) solution in CH_2Cl_2/MeOH under aerobic conditions with an excess of $Tl(OAc)_3$ (Scheme 1). The complex *trans*-Cd(N-NHCO(*o*-Cl)C_6H_4-tpp)(OAc) (**4**) was synthesized in 53% yield by reacting **2** with excess $Cd(OAc)_2$ in CH_3CN under aerobic conditions (Scheme 1). The molecular frameworks are depicted in Fig. 1a for **3**·0.5H_2O and in Fig. 1b for **4**·CH_2Cl_2. The cadmium–nitrogen bond distances are comparable to those of Cd(1)–N(p) = 2.301(5) Å in Cd(*N*-NHCOC_6H_5-tpp)(OAc) [6]. The Cd···N(4) distance of 2.600(4) Å for **4** is longer than 2.301(5) Å but is significantly shorter than the sum of the van der Waals radii of Cd and N (3.15 Å) [3]. This longer Cd···N(4) contact in **4** may be viewed as a secondary intramolecular interaction. Most chemists seems to consider this secondary interaction between the metal ion and the fourth N as a weak bond in N-substituted porphyrin metal complexes [7,8] .

We adopt the plane of three strongly bound pyrrole nitrogen atoms [*i.e.*, N(1), N(2) and N(3)] for **3** and **4** as a reference plane, 3N. The geometry around Tl (III) (or Cd (II)) is a distorted square-based pyramid in which the apical site is occupied by a chelating bidentate OAc^- group in **3** (or **4**). In complex **3**, Tl (III) and N(5) are located on the same side at 1.18 and 1.26 Å from its 3N plane, but for complex **4**, Cd (II) and N(5) are located on different sides at 1.06 and −1.55 Å from its 3N plane. Apparently, chelating bidentate OAc^- in **3** is *cis* to the (*o*-Cl)BA group with O(2) and O(3) being located separately at 2.95 and 3.13 Å out of the 3N plane, and bidentate OAc^- in **4** is *trans* to the (*o*-Cl)BA group with O(2) and O(3) located at 3.21 and 2.85 Å out of the 3N plane.

The N(4) pyrrole rings bearing the (*o*-Cl)BA group in **3** and **4** deviate mostly from the 3N plane, thus orienting separately with a dihedral angle of 47.6° and 30.8°, whereas small angle of 7.5°, 13.5° and 9.8° occur with N(1), N(2) and N(3) pyrrole for **3** and the corresponding angles are 21.8°, 1.4 ° and 17.0° with N(1), N(2) and N(3) pyrrole for **4**. In **3**, such a large deviation from planarity for the N(4) pyrrole is also reflected by observing a 16.2–20.3 ppm upfield shift of the C_β (C17, C18) at 115.4 ppm compared to 134.1 ppm for C_β (C2, C13), 134.1 ppm for C_β (C3, C12) and 131.6 ppm for C_β (C7, C8). In **4**, a similar deviation is also found for N(4) pyrrole by observing a 7.4–10.1 ppm upfield shift of C_β (C17, C18) at 124.0 ppm compared to 134.1 ppm for C_β (C3, C12), 134.0 ppm for C_β (C7, C8) and 131.4 ppm for C_β (C2, C13). The dihedral angles between the mean plane of the skeleton (3N) and the planes of the phenyl groups are 88.1° [C(24)], 54.1° [C(30)], 42.7° [C(36)] and 36.2° [C(42)] for **3** and the corresponding angles are 61.1°, 51.7°, 39.9° and 36.4° for **4**.

In solution, the molecule has effective C_s symmetry with a mirror plane running through the N(4)–N(5)–Tl(1)–N(2) unit for **3** and the N(2)–Cd–N(4)–N(5) unit for **4**. As a result, the ^{1}H NMR spectrum will exhibit four pyrrole resonances [H_β (2, 13), H_β (3, 12), H_β (7, 8), H_β (17, 18)] for these two complexes (Figs. 2 and 3). Fig. 2 depicts the representative ^{1}H spectra for **3** in CD_2Cl_2 at 20 and −90 °C. The NMR study of **3** showed three different types of Tl–H coupling constants for H_β. In **3** at 20 °C, the doublet at 9.30 ppm is assigned as H_β (2, 13) with ^4J(Tl–H) = 10.8 Hz and the other doublet at 8.59 ppm is due to H_β (7, 8) with ^4J(Tl–

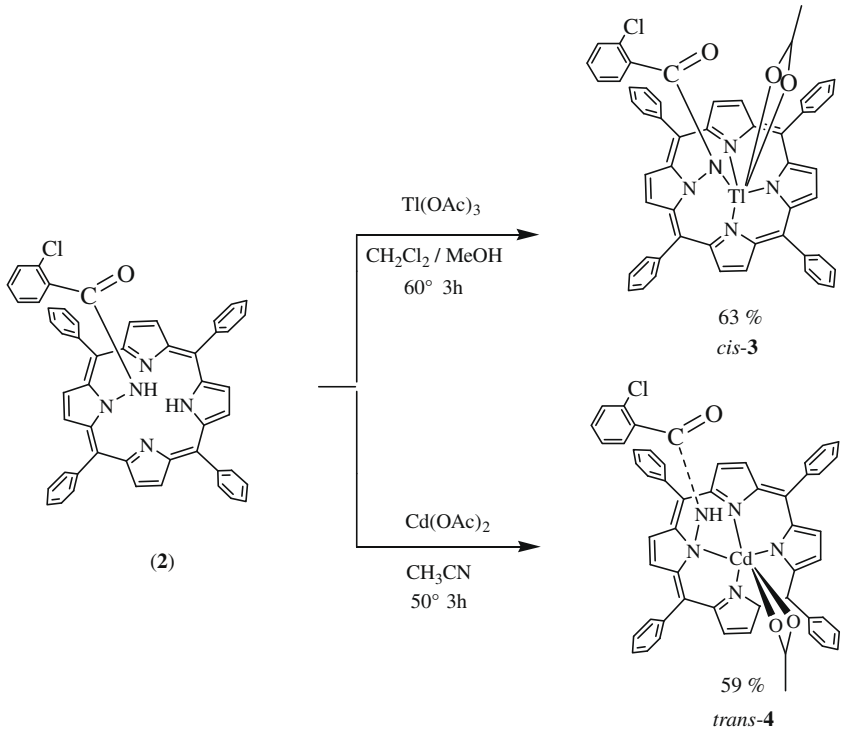

(**2**)

Scheme 1.

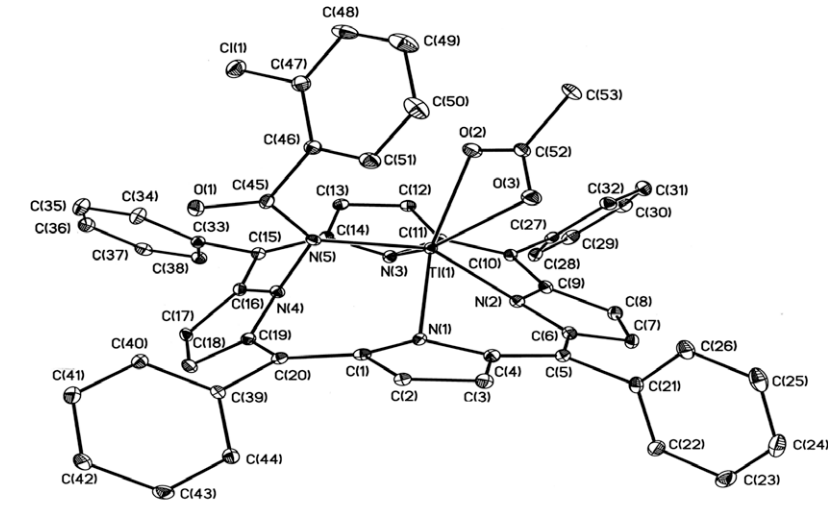

(a) **3** · $0.5H_2O$

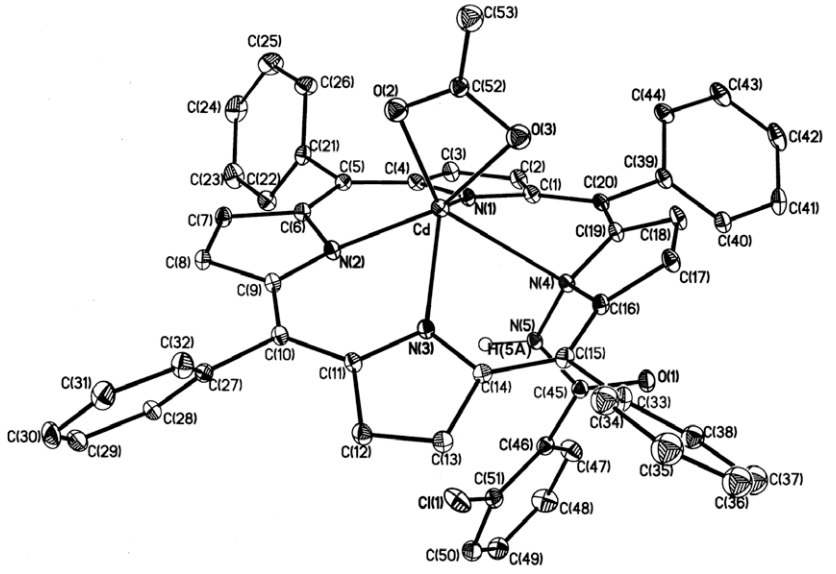

(b) **4** · CH_2Cl_2

Fig. 1. (a) Molecular structure of *cis*-Tl(N-NCO(*o*-Cl)C_6H_4-tpp)(OAc)·$0.5H_2O$ (**3**·$0.5H_2O$) and (b) *trans*-Cd(N-NHCO(*o*-Cl)C_6H_4-tpp)(OAc)·CH_2Cl_2 (**4**·CH_2Cl_2), with 30% thermal ellipsoids. Hydrogen atoms, solvent H_2O for **3**·$0.5H_2O$ and solvent CH_2Cl_2 for **4**·CH_2Cl_2 are omitted for clarity. Selected bond distances (Å): Tl(1)–N(1), 2.382(3); Tl(1)–N(2), 2.148 (3); Tl(1)–N(3), 2.350(3); Tl(1)–N(5), 2.131(3); Tl(1)–O(2), 2.299(3); Tl(1)–O(3), 2.432(3) for **3**·$0.5H_2O$; Cd–N(1), 2.294(4); Cd–N(2), 2.246(4); Cd–N(3), 2.331(4); Cd–O(2), 2.281(12); Cd–O(3), 2.344(10) for **4**?CH_2Cl_2 .

H) = 75.0 Hz. The singlet at 8.95 ppm is assigned to H_β (3, 12) and the other singlet at 7.26 ppm is due to H_β (17, 18) (Fig. 2a). In **4** at 20 °C, the doublet at 8.77 ppm is assigned to H_β (2, 13) with ^3J(H–H) = 4.2 Hz and the other doublet at 8.71 ppm with ^3J(H–H) = 4.2 Hz is due to H_β (3, 12) (Fig. 3a). The singlet at 8.81 ppm is assigned to H_β (7, 8) and the other singlet at 8.64 ppm is due to H_β (17, 18) (Fig. 3a).

The signal arising from the NH proton of **4** in CD_2Cl_2 was observed as a singlet at δ −0.99 ppm ($\Delta\nu_{1/2}$ = 13 Hz) at 20 °C. This NMR data suggests that the NH protons of **4** undergo intermediate intermolecular proton exchange with water at 20 °C. At low temperature the chemical exchange slows down that allows the observation of a broad singlet for the NH proton at −1.08 ppm ($\Delta\nu_{1/2}$ = 17 Hz) for **4** at −90 °C. In this case, the NH proton signal for **4** at −90 °C is broadened by the quadrupolar interaction of the ^{14}N nucleus.

Non-equivalence of the two sides of the macrocycle will cause each phenyl ring have two distinct *ortho* resonances, with one set of *ortho* protons, *o*-H (22, 32) [or *o*-H (26, 32)] and *o*-H (26, 28) [or *o*-H (22, 28)], for phenyl C(24) and C(30) and the other set of *ortho* protons, *o*′-H (34, 40) [or *o*′-H (34, 44)] and *o*′-H (38, 44) [or *o*′-H (38, 40)] for phenyl C(36) and C(42) of **3** (or **4**), respectively. In **3** at 20 °C, the rotation of the phenyl group along C_1–C_{meso} [C(5)–C(21) or C(10)–C(27)] bond is slow [9]. This slow rotation is supported by the two doublets at 8.25 and 8.12 ppm due to *o*-H (22, 32) and *o*-H (26, 28), respectively (Fig. 2a). Moreover, the rotation of phenyl group along C(15)–C(33) [or C(20)–C(39)] bond for **3** is at the near fast exchange region [9]. In this fast exchange region, the signals are observed as broad singlet at 8.47 ppm (Fig. 2a). At −90 °C, both rotations are extremely slow. Hence, the rate of intramolecular exchange of the *ortho* protons for **3** in CD_2Cl_2 is also extremely slow. The singlet at 8.16 ppm and the doublet at 8.13 ppm with ^3J(H–H) = 5.4 Hz is assigned as ortho protons *o*-H (26) and *o*-H (28). The two sets of signals at 8.27 and 8.20 ppm is due to *ortho* protons *o*-H (22) and *o*-H (32) for **3** (Fig. 2b). Likewise, the two partially overlapping doublets at 8.72 ppm with ^3J(H−H) = 7.8 Hz is

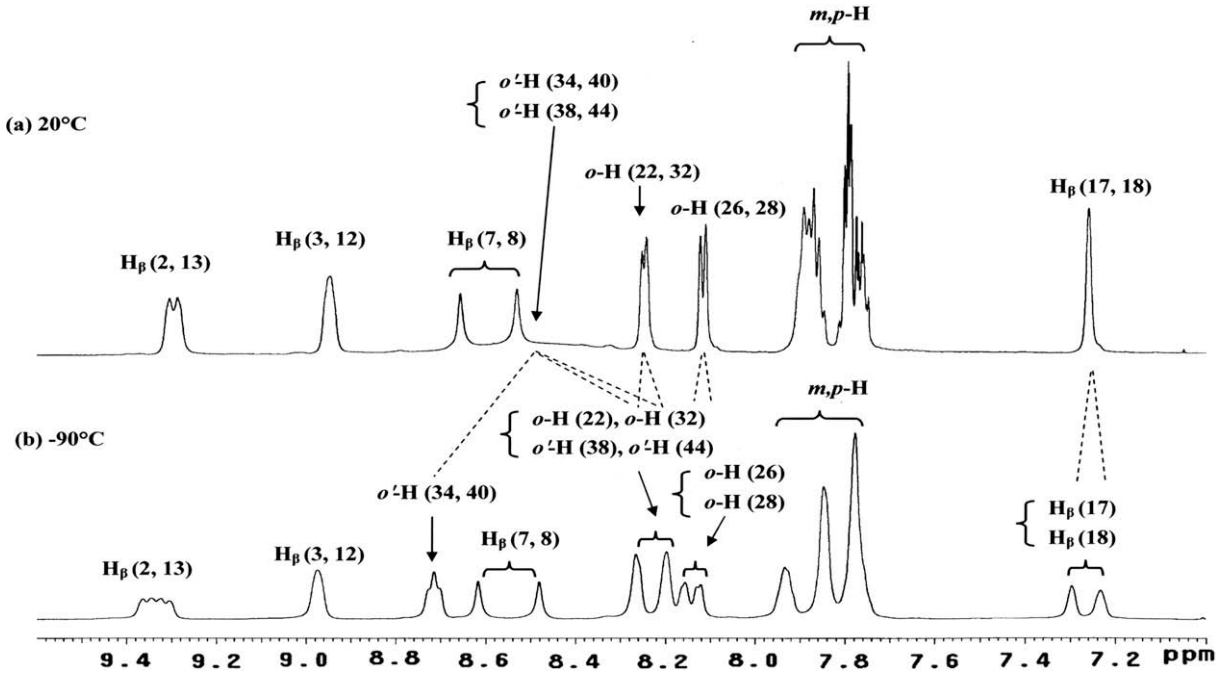

Fig. 2. ^{1}H NMR (599.95 MHz) spectra showing four different β-pyrrole protons H_β and phenyl protons (*o*-H, *m,p*-H) for **3** in CD_2Cl_2: (a) 20 °C and (b) −90 °C.

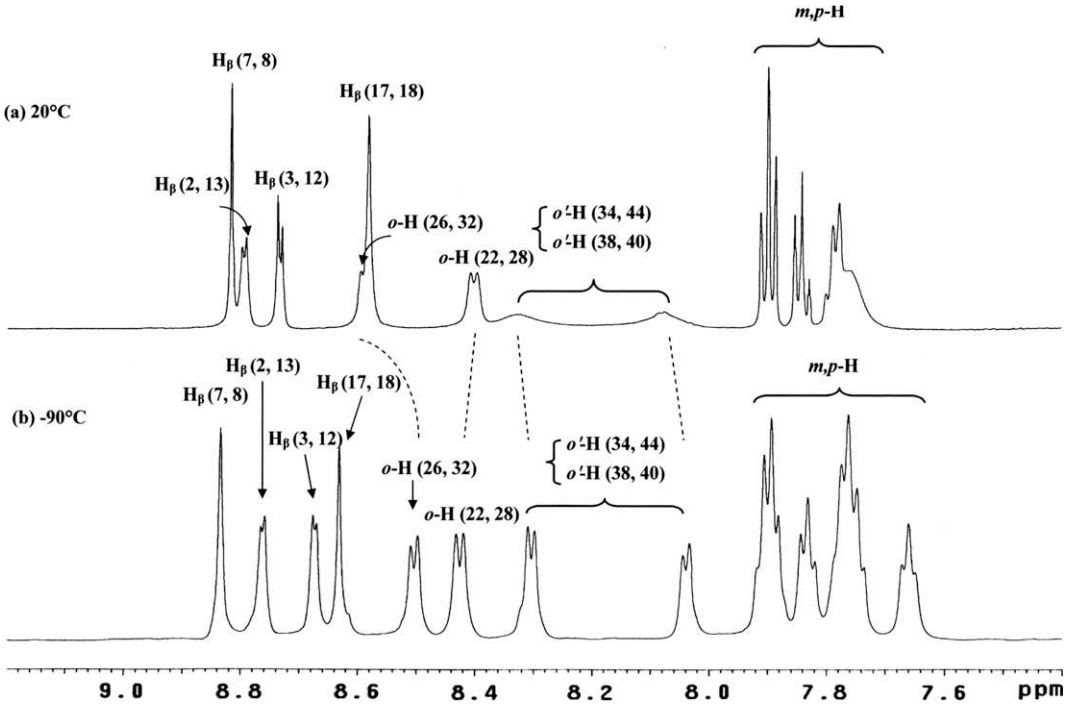

Fig. 3. ^{1}H NMR (599.95 MHz) spectra showing four different β-pyrrole protons H_β and phenyl protons (*o*-H, *m,p*-H) for **4**: (a) in $CDCl_3$ at 20 °C and (b) in CD_2Cl_2 at −90 °C.

due to *ortho* protons *o*′-H (34, 40). The same two sets of signals at 8.27 and 8.20 ppm is also due to ortho protons o′-H (38) and o′-H (44) for **3** (Fig. 2b). The free energy of activation $\Delta G^{\neq}_{293} = 55.94$ kJ/mol is therefore, determined for the intramolecular exchange of the *ortho* protons between *o*′-H (34, 40) and *o*′-H (38, 44) in **3**.

In a similar fashion, the rotation of the phenyl group of **4** in $CDCl_3$ at 20 °C along C(10)–C(27) [or C(5)–C(21)] bond is slow and the rotation along C(20)–C(39) [or C(15)–C(33)] is at the intermediate exchange region [9]. Hence the ^{1}H resonances for the *ortho* protons of **4** in $CDCl_3$ at 20 °C were observed as two sets of doublets: one doublet at 8.65 ppm is assigned to *ortho* protons *o*-H (26, 32) with ^3J(H–H) = 6.6 Hz and the other doublet at 8.44 is due to *ortho* protons *o*-H (22, 28) with ^3J(H–H) = 6.6 Hz (Fig. 3a). Likewise, two sets of broad singlet at 8.37 and 8.08 ppm is due to *ortho* protons *o*′-H (34, 44) and *o*′-H (38, 40) (Fig. 3a). However, for *ortho* protons of **4** in CD_2Cl_2 at −90 °C, the rotation of phenyl group along C_1–C_{meso} bond in **4** is extremely slow, which is evident from the appearance of the four doublets at 8.49 [*o*-H (26, 32)],

8.42 [*o*-H (22, 28)], 8.31 and 8.04 ppm for *o*′-H (34, 44) and *o*′-H (38, 40) due to four different *ortho* protons of the aromatic ring in **4** (Fig. 3b).

Due to the ring current effect, upfield shifts for the ^{1}H resonances of (*o*-Cl)BA-Ph-H_6, (*o*-Cl)BA-Ph-H_3, (*o*-Cl)BA-Ph-H_5 and (*o*-Cl)BA-Ph-H_4 for **4** in $CDCl_3$ at 20 °C are $\Delta\delta = -3.2$ [from 7.77 (obtained from *o*-chlorobenzamide) to 4.57 ppm], −1.46 (from 7.42 to 5.96 ppm), −1.34 (from 7.35 to 6.01 ppm) and −1.08 (from 7.40 to 6.32 ppm), respectively. As the distance between the geometrical center (C_t) of the 4N plane [*i.e.*, N(1), N(2), N(3), N(4) for **3** and **4**] and axial protons gets smaller, the shielding effect becomes larger. In **4**, the distance for $C_t\cdots$(*o*-Cl)BA-Ph-H_6, $C_t\cdots$(*o*-Cl)BA-Ph-H_3, $C_t\cdots$(*o*-Cl)BA-Ph-H_5 and $C_t\cdots$(*o*-Cl)BA-Ph-H_4, increases from 5.419, 6.284, 7.057 to 7.396 Å. As the (*o*-Cl)BA-Ph-H_6 proton of **4** is closer to C_t, the shielding gets larger for this (*o*-Cl)BA-Ph-H_6 protons. A similar ring current effect is also observed for **3**. The average distance between $C_t\cdots$(*o*-Cl)BA-Ph-H_6, $C_t\cdots$(*o*-Cl)BA-Ph-H_5, $C_t\cdots$(*o*-Cl)BA-Ph-H_3 and $C_t\cdots$(*o*-Cl)BA-Ph-H_4 for **3** increases from 3.233, 4.866, 5.946 to 5.984 Å. The ^{1}H NMR spectra reveal that the aromatic protons of the (*o*-Cl)BA group appear as a doublet of triplets at 6.36 ppm [(*o*-Cl)BA-Ph-H_4], a doublet at 6.21 ppm [(*o*-Cl)BA-Ph-H_3], the triplet at 6.10 ppm [(*o*-Cl)BA-Ph-H_5] and the other doublet at 4.87 ppm [(*o*-Cl)BA-Ph-H_6] for **3**. The (*o*-Cl)BA bonding argument is further supported by the result that at 20 °C in ^{13}C NMR the (*o*-Cl)BA-Ph-C_1 [*i.e.*, C(46)] and the C(45) peaks in **3** were observed at 132.6 ppm with ^3J(Tl–C) = 20.1 Hz and at 167.7 ppm with ^2J(Tl–C) = 665 Hz, respectively.

The ^{1}H NMR spectrum for OAc^- of **4** in CD_2Cl_2 displays a sharp singlet for CH_3 at δ 0.06 ppm with $\Delta\nu_{1/2}$ = 3 Hz at 20 °C and remains a sharp singlet for the same methyl proton at δ −0.01 ppm with $\Delta\nu_{1/2}$ = 4 Hz at −90 °C. This minimum deviation in the value of line width ($\Delta\nu_{1/2}$) upon cooling indicates that OAc^- exchange does not occur in compound **4**.

Upon cooling of a 0.02 M CD_2Cl_2 solution of **3**, the methyl proton signal of OAc^-, being a single peak at 20 °C (δ 0.17 ppm), first broadened (coalescence temperature $T_c = -75$ °C) and then split into peaks with a separation of 14.4 Hz at δ 0.08 ppm at −90 °C. As the exchange of OAc^- within **3** is reversible, the results at 599.95 MHz confirm the separation as a coupling of ^4J(Tl–H) rather than a chemical shift difference [10,11]. The most likely cause of loss of coupling is due to the reversible dissociation of acetate with a small dissociation constant.

$$\mathrm{Tl}(\textit{N}\text{-NCO}(\textit{o}\text{-Cl})\mathrm{C_6H_4}\text{-tpp})(\mathrm{OAc}) \overset{\mathrm{CD_2Cl2}}{\rightleftharpoons} \mathrm{Tl}(\textit{N}\text{-NCO}(\textit{o}\text{-Cl})\mathrm{C_6H_4}\text{-tpp})^+ + \mathrm{OAc}^- \quad (1)$$

Such a scenario would lead to the change in the chemical shift with temperature and no detectable free OAc^- and Tl(*N*-NCO(*o*-Cl)C_6H_4-tpp)$^+$ at low temperature, but would lead to the loss of coupling between acetate and thallium at higher temperature [10–12]. The chemical shift in the high-temperature limit is the average of the two species (*i.e.*, Tl(*N*-NCO(*o*-Cl)C_6H_4-tpp)(OAc) and OAc^-) in Eq. (1) weighted by their concentration. The free energy of activation at the coalescence temperature T_c for the intermolecular exchange of OAc^- in **3** is determined to be $\Delta G^{\neq}_{198} = 42.1$ kJ/mol. At 20 °C, intermolecular exchange of the OAc^- group for **3** is rapid as indicated by the appearance of singlet signals due to carbonyl carbons at 175.0 ppm and methyl carbons at 18.5 ppm. At −90 °C, the rate of intermolecular exchange of OAc^- for **3** in CD_2Cl_2 is slow. Hence, at this temperature, the methyl and carbonyl carbons of OAc^- are observed at 17.5 ppm [with ^3J(Tl–C) = 200 Hz] and 174.7 ppm [with ^2J(Tl–C) = 204 Hz] as doublets, respectively [11].

X-ray diffraction analysis unambiguously confirms that **3** and **4** have a chelating bidentate OAc^- ligand in the solid state. The ^{13}C NMR chemical shifts were shown to be a useful tool for diagnosing the nature of acetate ligands, whether unidentate or bidentate in diamagnetic complexes. Unidentate acetate ligands were located at 20.5 ± 0.2 and 168.2 ± 1.7 ppm and bidentate acetate ligands at 18.0 ± 0.7 and 175.2 ± 1.6 ppm [13]. The methyl and carbonyl chemical shifts of the acetate group in **3** (or **4**) at 20 °C in $CDCl_3$ are separately located at 18.5 (or 18.9) and 175.0 (or 176.4) ppm confirming that the acetate is chelating bidentately and is coordinated to the thallium (or cadmium) atom in **3** (or **4**) in the solution phase.

In conclusion, we have investigated two new, diamagnetic and mononuclear porphyrin complexes, namely, a thallium(III) complex **3**·0.5H_2O and a cadmium(II) complex **4**·CH_2Cl_2 and their X-ray structures are established. In **3**, the N–H bond of the *o*-chlorobenzamido ligand is cleaved and the *o*-chlorobenzamido nitrogen participates in bonding to the thallium ion. Complex **3** is a bridged metalloporphyrins with a metal–N–N linkage. In **4**, the (*o*-Cl)BA substituent is left intact and the cadmium(II) ion is coordinated to the four nitrogens [N(1)–N(4)] of the macrocycle core. Compound **4** is a cadmium(II) N-substituted-N-aminoporphyrin complex.

Acknowledgments

The financial support from the National Research Council of the ROC under Grant NSC 98-2113-M-005-005 is gratefully acknowledged. We thank Dr. S. Elango for helpful discussions.

Appendix A. Supplementary material

CCDC 695921 (for **3**·0.5H_2O) and 695922 (**4**·CH_2Cl_2) contain the supplementary crystallographic data for this paper. These data can be obtained free of charge from The Cambridge Crystallographic Data Centre via www.ccdc.cam.ac.uk/data_request/cif. Supplementary data associated with this article can be found, in the online version, at doi:10.1016/j.inoche.2010.01.022.

References

[1] C.Y. Chen, H.Y. Hsieh, J.H. Chen, S.S. Wang, J.Y. Tung, L.P. Hwang, Polyhedron 26 (2007) 4602.
[2] R.G. Pearson, Inorg. Chem. 27 (1988) 734.
[3] J.E. Huheey, E.A. Keiter, R.L. Keiter, Inorganic Chemistry, fourth ed., Harper Collins College Publishers, New York, 1993. pp. 114, 292.
[4] Y. Zhang, Inorg. Chem. 21 (1982) 3886.
[5] Y. Zhang, Inorg. Chem. 21 (1982) 3889.
[6] F.A. Yang, J.H. Chen, H.Y. Hsieh, S. Elango, L.P. Hwang, Inorg. Chem. 42 (2003) 4603.
[7] J.Y. Tung, J.H. Chen, Polyhedron 26 (2007) 589.
[8] M. Ravikanth, T.K. Chandrashekar, Struct. Bond. 82 (1995) 105.
[9] R.S. Drago, Physical Methods for Chemists, second ed., Saunder College Publishing, New York, 1992. pp. 290–295.
[10] J.Y. Tung, J.I. Jang, C.C. Lin, J.H. Chen, L.P. Hwang, Inorg. Chem. 39 (2000) 1106.
[11] F.A. Yang, K.Y. Cho, J.H. Chen, S.S. Wang, J.Y. Tung, H.Y. Hsieh, F.L. Liao, G.H. Lee, L.P. Hwang, S. Elango, Polyhedron 25 (2006) 2207.
[12] J.P. Jenson, E.L. Muetteries, in: L.M. Jackman, F.A. Cotton (Eds.), Dynamic Nuclear Magnetic Resonance Spectroscopy, Academic Press, New York, 1975, pp. 299–304.
[13] S.J. Lin, T.N. Hong, J.Y. Tung, J.H. Chen, Inorg. Chem. 36 (1997) 3886.